

## Sintering and characterization of PLZT (9/65/35)

M. Cerqueira <sup>a</sup>, R.S. Nasar <sup>a,\*</sup>, E.R. Leite <sup>b</sup>, E. Longo <sup>b</sup>, J.A. Varela <sup>c</sup>

<sup>a</sup>Departamento de Química, Universidade Federal do Rio Grande do Norte, PO Box 1662, Natal, RN, 59078-970, Brazil

<sup>b</sup>Departamento de Química, UFSCar, São Carlos, SP, 13565-905, Brazil

<sup>c</sup>Instituto de Química, UNESP, Araraquara, SP, 14800-900, Brazil

Received 20 November 1998; received in revised form 26 February 1999; accepted 3 June 1999

### Abstract

PLZT(9/65/35) obtained by association between the Pechini method (ZT) and partial oxalate (PLZT) was prepared. The stoichiometric phase and monophasic (cubic) PLZT obtained by calcination did not occur after sintering. The sintering process, by using two stages, caused a liquid phase formation due to a PbO excess (5 and 10 wt%). Samples with high density ( $\sim 8 \text{ g/cm}^3$ ) and optical transparency ( $\sim 12\%$ ) were obtained. However, an equilibrium between the excess of PbO of sample/atmosphere PbO leads to a segregated PbO phase on the boundaries of the microstructure. A diffusion of Zr, Ti and La ions from PLZT to PbO phase promoted a stoichiometric deviation of the matrix and modified the optical and dielectric characteristics. © 2000 Elsevier Science Ltd and Techna S.r.l. All rights reserved.

**Keywords:** Synthesis; Pechini process; Zirconium titanate;  $\text{ZrTiO}_4$ , La containing PZT (PLZT)

### 1. Introduction

It is known that certain additions of lanthanum in lead zirconate titanate, PZT modifies its properties from ferroelectric transducer to electrooptic characteristics [1].

Despite the fact that PZT is ferroelectric, with structures such as tetragonal ( $F_T$ ) and/or rhombohedral ( $F_R$ ), the high optical transparency of PLZT is due to its paraelectric cubic structure ( $P_C$ ).

It is accepted that the lanthanum addition causes a distorted effect in the unit cell. This reduces the optical anisotropy in the crystalline lattice and leads to a growth of uniform grains, only one dense phase and promotes a free porous structure [2,3].

A relation exists between the lanthanum concentration in the lattice, and the zirconium/titanium concentration. Increases of titanium concentration needs an increase in the lanthanum concentration to obtain an electrooptic effect of PLZT ceramics [4].

PZT and PLZT are dependents of the homogeneity [5] of additive concentration [6] and of the microstructure [7]. The influence of these variables is dependent on the processing, quality and the type of precursors. As a highly homogeneous method, Pechini [8] developed a

polymeric resin starting with a citrate synthesis and a polymerization with ethyleneglycol.

Other authors [9–11] prepared and characterized the zirconium titanate (ZT) by the Pechini method, and lead zirconate titanate (PZT) and lead lanthanum titanate zirconate (PLZT) by the Pechini (ZT) and the partial oxalate method (PLZT).

PbO excess added during sintering, when correctly processed, increases the densification of ceramic bodies. PbO excess leads to a liquid phase formation on the grain boundaries in the initial stage of sintering, and promotes a rapid densification process, and obtains values near to the theoretical density. This effect decreases the residual porosity that occurs on the contours of the microstructure [12].

In the present work the sintering process and the electric and transparency characteristics, such as the dielectric constant and the visible-UV transmission of PLZT(9/65/35) was studied.

### 2. Experimental procedures

#### 2.1. Processing

##### 2.1.1. Synthesis

The  $\text{ZrTiO}_4$  (ZT) phase was prepared by the polymeric precursor method [9,10] with the Zr/Ti stoichiometric

\* Corresponding author. Tel.: +55-84-215-3823; fax: +55-84-211-9224.  
E-mail address: nasar@zaz.com.br (R.S. Nasar).

ratio of 65/35, calcined at 800°C for 3 h and then suspended with an oxalic acid solution (99.9% Merck, Germany) with the same molar equivalent of lead nitrate,  $\text{Pb}(\text{NO}_3)_2$  and lanthanum oxide,  $\text{La}_2\text{O}_3$ . This solution of  $\text{Pb}(\text{NO}_3)_2$  and lanthanum oxide was dripped into an ammoniac solution of oxalic acid where a precipitation of lead oxalate and lanthanum oxide occurred on the surface of the ZT particles at  $\text{pH}=12$ . The powder mixture was calcined at 800°C for 5 h.

### 2.1.2. Sintering

Two lots of powder with 5 wt% (PLZT.5P) and 10 wt% (PLZT.10P) of PbO excess were prepared. Pellets with a mass of 1 g and a diameter of 1.25 cm were pressed isostatically at 150 MPa. Two stages of sintering occur: in the first stage the pellets were sintered at temperatures between 900 and 1150°C for 2 h in a platinum crucible in an atmosphere of oxygen and buried in PLZT powder. In the second sintering stage, the high density samples of PLZT.5P (5% PbO excess) were sintered at 1100°C for 12 and 22 h and the PLZT.10% (10% PbO excess) samples sintered at 1050°C for 2, 12 and 22 h in alumina crucibles with PLZT as an atmosphere powder. The calcined powder at 800°C for 5 h and pellets sintered at 1100°C for 12 h after the second sintering stage were analyzed by X-ray diffraction pattern (XRD). A SIEMENS diffractometer with  $\text{CuK}\alpha$  radiation (Model D-5000) and graphite monochromator was used.

### 2.1.3. Rietveld method

This method consists of a comparison between a calculated X-ray diffraction pattern [13] that used defined crystallographic parameters and an experimental spectrum.

Experimental peaks were obtained by using a step by step scanning process with constant increment and time.

For a multiphase analysis, an equation such as the following is obtained:

$$Y_{ec} = \sum_h J_h L P_h F^2 G(\Delta\theta_{ih}) P_h + Y_{bi}$$

S = scale factor,

$J_h$  = multiplicity,

L = lorentz factor,

$P_h$  = polarization factor,

F = structure factor,

$\Delta\theta$  =  $i^{\text{th}}$  angle,

$Y_{bi}$  = next peak contributions

An approximation between the observed X-ray diffraction and the calculations were made by minimum squares with the use of a Lorentzian type curve.

New refined parameters were obtained by using a calculated X-ray diffraction profile. Both the refined profile and the phases deconvolution were obtained from the peaks of the X-ray diffractogram.

## 2.2. Microscopy

### 2.2.1. Optical microscopy

Samples of different PbO compositions were polished with alumina 0.1 and 1  $\mu\text{m}$ . Analysis of different phases of sintered powders was carried out by a polarized light microscopy with the use of a JEOL JSM-T 330 A microscopy.

### 2.2.2. Microanalysis by EDS

After the second sintering stage the microstructure was observed and a qualitative chemical analysis was carried out. Scanning electron microscopy (SEM) (Leica/Cambridge 440 stereoscan) and a microanalysis apparatus Link/OXFORD-EDX model was used.

## 2.3. Dielectric constant

Gold electrodes at the sample surface were applied. Capacitance at temperatures from 20 to 350°C at 100 kHz were measured. The dielectric constant, by using the capacitance data was calculated. A HP 4194 impedance analyzer was used.

## 2.4. Light transmission

After the second sintering stage, samples were polished to 0.2 mm thickness, and analyzed in the visible-UV region (390–770 nm) by transmission measures. A diode array spectrophotometer HP 8452 A equipment was used.

## 3. Results

### 3.1. Phases formation

Fig. 1 shows the XRD pattern of calcined powder at 800°C/5 h of ZT-PbC<sub>2</sub>O<sub>4</sub>-La<sub>2</sub>O<sub>3</sub> [10] mixture. A monophasic PLZT (9/65/35) which has  $P_c$  structure was obtained.

Samples sintered at 1200°C/2 h (platinum crucible) during the first sintering stage, Fig. 2 shows the appearance of other phases, such as,  $F_R$  and  $F_T$ . XRD

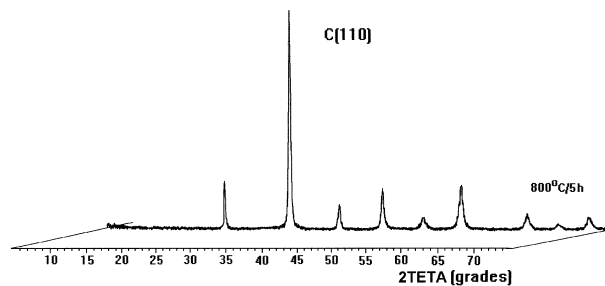


Fig. 1. X-ray diffraction pattern of PLZT calcined at 800°C/5 h. (C: cubic phase).

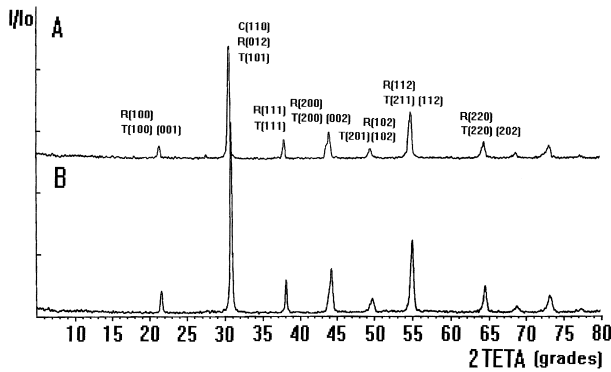


Fig. 2. X-ray diffraction pattern of sintered PLZT after the second sintering Y stage, (A) PLZT.5P; (B) PLZT.10P, (C: cubic phase, T: tetragonal phase, R: rhombohedral phase).

pattern, after the second sintering stage (alumina crucible) shows that the phases are the same. Coexistence occurs between the  $F_T$  and  $F_R$ , which are ferroelectric phases and the  $P_c$  non-ferroelectric phase. This indicated that, after the calcination, the use of PbO excess addition caused a stoichiometric deviation ( $P_c \rightarrow F_T$  and  $F_R$ ).

### 3.2. Loss of mass

In the first sintering stage a high activity of the loss of mass, Table 1, was observed. PbO loss of the structure of stoichiometric composition (PLZT) occurs. Apparent densities of samples of about 7.8 g/cm<sup>3</sup> (PLZT), 7.85 g/cm<sup>3</sup> (PLZT.5P) at 1100°C and 8.15 g/cm<sup>3</sup> (PLZT.10P) at 1050°C were obtained.

Table 2 shows the loss of mass after the second sintering stage, which demonstrated that about 12 h were necessary for equilibrium between the PbO of samples/atmospheric PbO, to occur (PLZT.5P and 10P).

### 3.3. Microscopy and microanalysis by EDS

Fig. 3(a) and (b) shows samples of the photographs of polarized light microscopy with the presence of another phase after the second sintering stage. Large precipitates

Table 1  
Loss of mass at the first sintering stage

Temp. (°C) 2 h	PLZT (%)	PLZT.5P (%)	PLZT.10P (%)
1050	1.43	4.03	6.30
1100	1.82	4.16	6.30

Table 2  
Loss of mass at the second sintering stage

Time/h	PLZT.5P (%)	PLZP.10P (%)
2	5.57	7.80
12	6.73	8.80
22	5.92	8.80

of the PLZT.10P samples were observed, possibly caused by the liquid phase excess during the sintering.

Analysis by SEM, Fig. 3(c) and (d), shows a high precipitate concentration on the surface of the samples of both PLZT.5P and 10P.

Fig. 4 shows a microanalysis by EDS of precipitates of PLZT.5P and PLZT.10P with the presence of Pb, Ti, Zr and La with high Pb concentration. This analysis confirmed the XRD results that showed a non-stoichiometric PLZT was formed after the second sintering stage.

### 3.4. Dielectric constant

Fig. 5 shows the relative dielectric constant, after the first sintering stage, of different compositions. Sintering of PLZT occurs by solid state reaction with a loss of mass and vacancies formation in the perovskite structure. Both PLZT.5P and 10P shows a high activity of loss of mass. However, a strong rearrangement of the microstructure of PLZT.10P due to a liquid phase of PbO increases the density and shows values of dielectric constant of 11 000 and a Curie point of 170°C typical of concentrations below 9 mol% of La<sub>2</sub>O<sub>3</sub> [1].

### 3.5. Transmission

Fig. 6 shows the transmission of PLZT.5P and 10P in the visible-UV region after the second sintering stage with values of about 6.2 and 11.8%, respectively. The presence of precipitates in the second phase caused a decrease in the transmission of the samples. Transmissions are according to the density values of 8.20 g/cm<sup>3</sup> (PLZT.5P) and 7.95 g/cm<sup>3</sup> (PLZT.10P).

## 4. Discussion

Recent papers in the literature showed that the Pechini method [9,10] and partial oxalate [11] promoted the formation of a monophase PLZT powder with high surface area.

According to results, a non-equilibrium reaction during the sintering, caused a non-stoichiometric PLZT formation due to a slow equilibrium between PbO of sample/atmospheric PbO, (Table 2) that caused PbO segregation. After the equilibrium, a PbO phase at the grain boundaries sequestered Zr, Ti and La ions of the matrix and formed a non-stoichiometric  $F_T$  and  $F_R$  phase on the contours of the microstructure.

Excess of the liquid phase in the PLZT.10P at the initial sintering stage leads to density increases due to a rearrangement of microstructure. A remnant liquid phase in the grain boundaries, after the first sintering stage, increased the capacitance in the grains due to high defect concentrations near to the grain boundaries. A consequential increase of the Curie temperature due

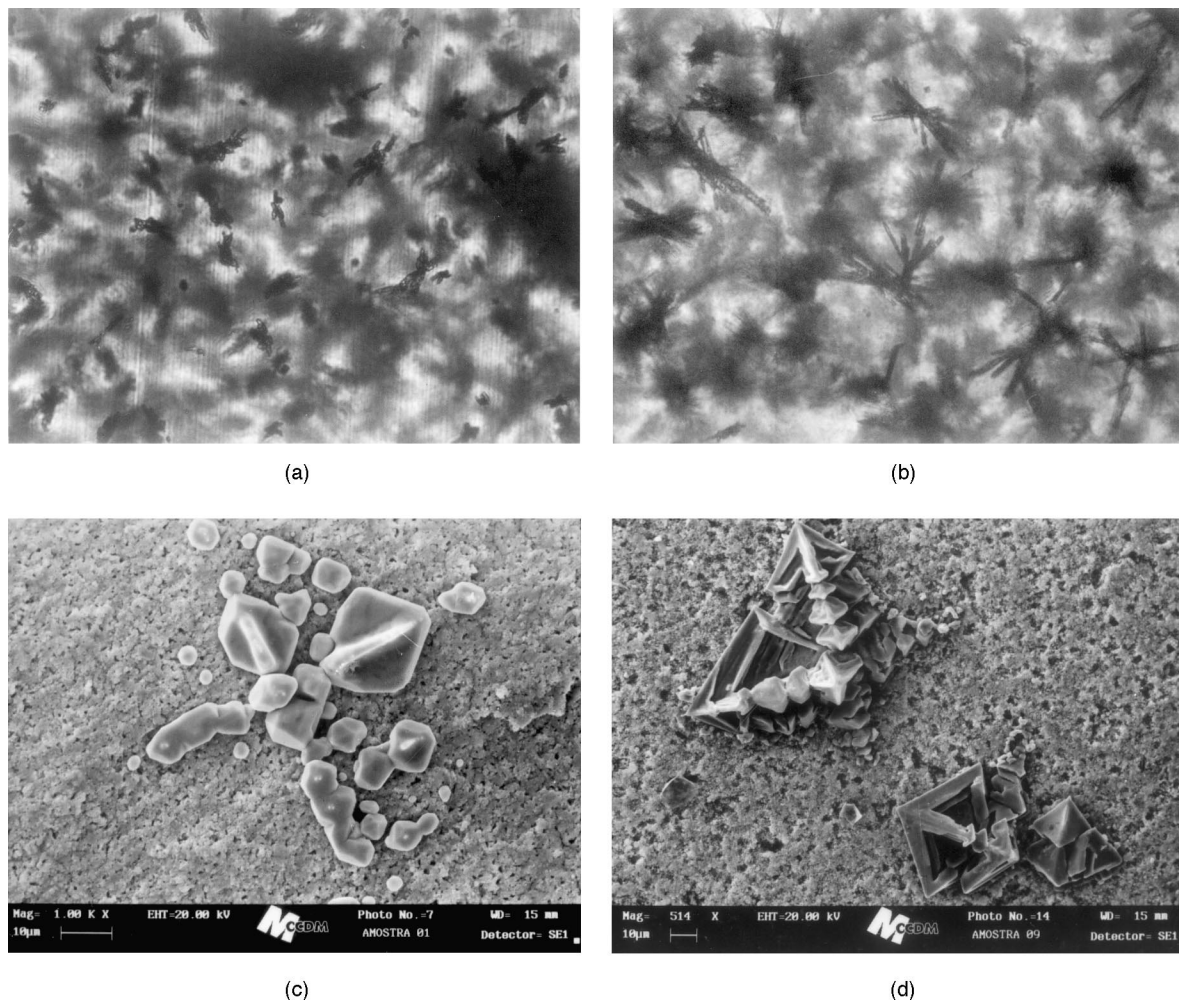


Fig. 3. Photographs of polarized light microscopy and SEM of the PLZT precipitates. (a) PLZT.P, 1100°C/12 h (x 400); (b) PLZT.10P, 1100°C/12 h (x 400); (c) PLZT.5P, 1100°C/12 h (SEM); (d) PLZT.10P, 1100°C/12 h (SEM).

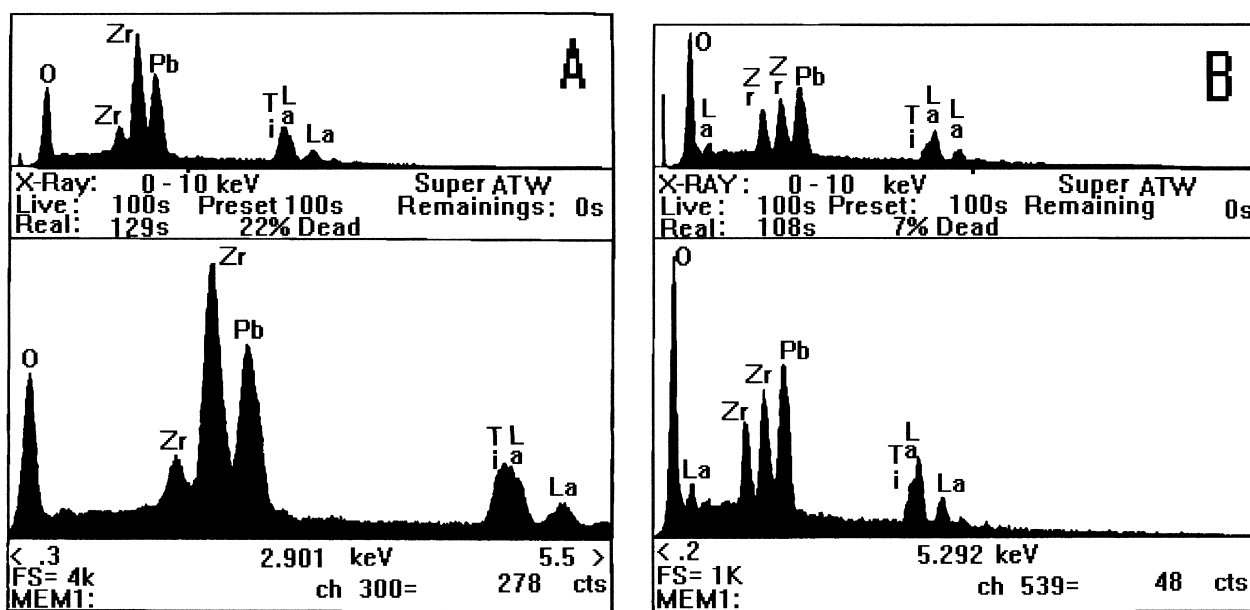


Fig. 4. Microanalysis by EDS of precipitates of PLZT sintered at 1100°C/12 h. (A) PLZT.5P; (B) PLZT.10P.

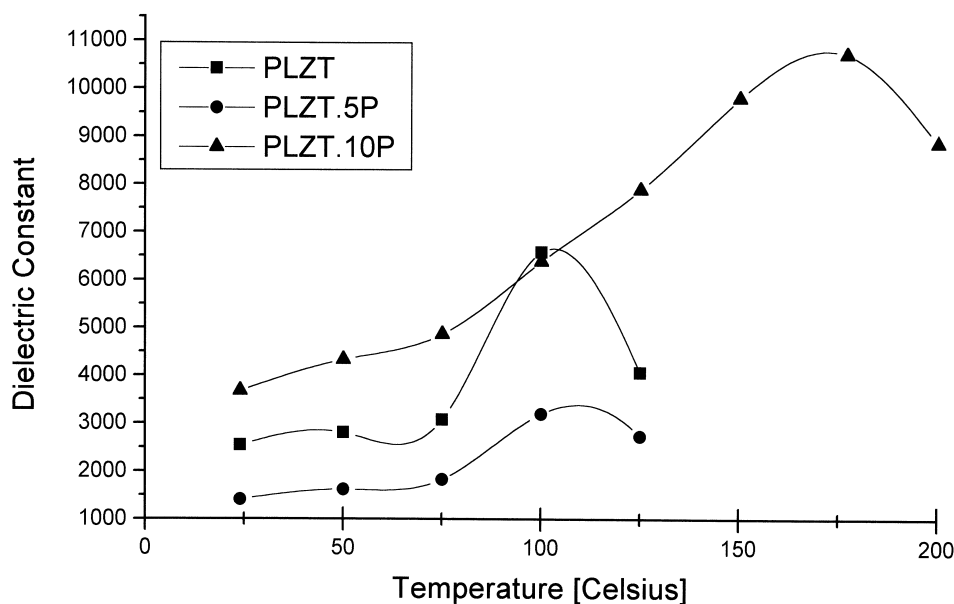


Fig. 5. Relative dielectric constant of PLZT after the first sintering stage.

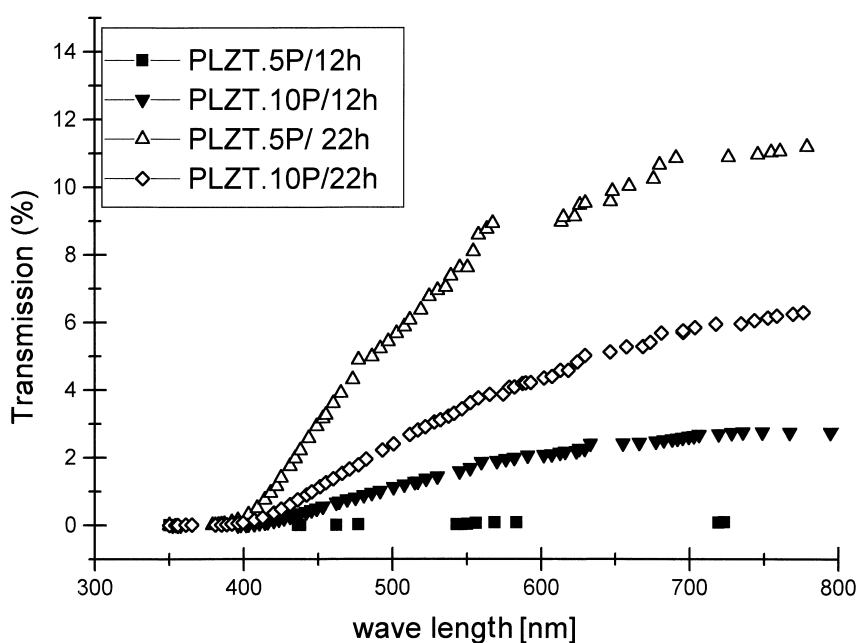


Fig. 6. Transmission of PLZT in the visible-UV region after the second sintering stage.

to the ferroelectric phase's presence occurs. The PLZT phases, with ferroelectric characteristics, have  $F_T$  and  $F_R$  structures due to a minor lanthanum concentration and has domain walls that present high dielectric constants. Low densities of PLZT samples and a small liquid phase presence in the PLZT.5P demonstrate coherent results of dielectric measures.

The paraelectric cubic phase presence promoted the light transmission at the visible-UV region of PLZT.5P samples. A decrease in the optic characteristics of the electrooptic phase were due to the presence of second

phase precipitates with  $F_R$  and  $F_T$ , that have domain walls which lead to light deviation by scattering.

## 5. Conclusions

The synthesis of PLZT (9/65/35) by the Pechini method and partial oxalate allows the formation of monophasic ( $P_C$ ) PLZT. A non-equilibrium condition between PbO of sample/atmospheric PbO causes a PbO segregation which sequesters Ti, Zr and La ions and

form a new phase on contours of the microstructure. The rearrangement of the microstructure and a precipitate concentration with domain walls leads to alterations of the dielectric constant and of light transmission of the samples.

## References

- [1] G.H. Haertling, *Ceramic Materials for Electronics*, Dekker, New York, 1986, p. 157.
- [2] S.K. Saha, D.C. Agrawal, *Am. Ceram. Soc. Bull.* 71 (1992) 1424.
- [3] G.H. Haertling, *Ceramic Materials for Electronics*, Dekker, New York, 1986, p. 168.
- [4] K. Oshima, K. Tsuzuki, *Jpn. J. Appl. Phys.* 33 (1994) 5389.
- [5] K. Kakegawa, L. Mohri, T.H. Takahashi, S. Shirasaki, *Solid State Commun.* 24 (1977) 769.
- [6] R. Gerson, *J. Appl. Phys.* 31 (1960) 188.
- [7] J.F.F. Lozano, C. Moure, *Bol. Soc. Esp. Vidr.* 227 (1988) 17.
- [8] M. Pechini, U.S. Patent no. 3.330.697, 1967.
- [9] M. Cerqueira, R.S. Nasar, E. Longo, E.R. Leite, J.A. Varela, *Mater. Lett.* 22 (1995) 181.
- [10] E.R. Leite, M. Cerqueira, M. Perazoli, R.S. Nasar, E. Longo, J.A. Varela, *J. Am. Ceram. Soc.* 79 (1996) 1563.
- [11] M. Cerqueira, R.S. Nasar, E.R. Leite, E. Longo, J.A. Varela, *Mater. Lett.* 35 (1998) 166.
- [12] L. Eyraud, P. Eyraud, P. Gonnard, P. Troccaz, *Ferroelectrics* 34 (1981) 133.
- [13] C.J. Howard, R.J. Hill, *J. Mater. Sci.* 26 (1991) 17.